Unconventional multicritical point in the $S = \frac{1}{2}$ Re_2-cluster magnet $La_3Re_2O_{10}$

Yuya Haraguchi,[1] Chishiro Michioka,[1] Hiroaki Ueda,[1] and Kazuyoshi Yoshimura[1,2]
[1]*Department of Chemistry, Graduate School of Science, Kyoto University, Kyoto 606-8502, Japan*
[2]*Research Center for Low Temperature and Materials Sciences, Kyoto University, Kyoto 606-8502, Japan*
(Received 4 May 2014; revised manuscript received 27 June 2014; published 5 August 2014)

Magnetic properties were investigated in $La_3Re_2O_{10}$ with Re_2 clusters. An Re_2 cluster has three $5d$ electrons in nondegenerated cluster orbitals, resulting in the construction of $S = 1/2$ spin per Re_2 cluster. $La_3Re_2O_{10}$ has a Weiss temperature of approximately -110 K and exhibits a broad maximum in the temperature dependence of magnetic susceptibility, suggesting the development of short-range ordering among cluster spins at low temperatures. $La_3Re_2O_{10}$ shows an antiferromangetic ordering at $T_N = 18.7$ K, and below T_N, $La_3Re_2O_{10}$ shows a strong field dependence of magnetization, which indicates several phase transitions. The magnetic properties of $La_3Re_2O_{10}$ are summarized as a magnetic field-temperature phase diagram, which suggests an unconventional multicritical point. Such a phenomenon cannot be interpreted only by the magnetic interactions owing to phase rule, suggesting the existence of other degrees of freedom for making an exotic phase transition.

DOI: 10.1103/PhysRevB.90.064403 PACS number(s): 64.60.Kw, 75.30.Kz, 75.47.Lx

I. INTRODUCTION

Generally, a cluster of transition-metal ions often has molecular-orbital-like cluster orbitals. When there are unpaired spins in cluster orbitals, the cluster shows characteristics similar to a magnetic ion. Such magnetic clusters are attractive as a macroscopic localized moment system consisting of microscopic intercluster itinerant electrons by a transfer of d electrons in the cluster. Thus these magnetic metal clusters often produce unusual magnetic properties in the intermediate research field between localized and itinerant electron systems [1–6]. For example, GaV_4S_8 with V_4 tetrahedral clusters shows an unconventional structural phase transition owing to the orbital degree of freedom in a cluster orbital [1,2]. In addition, itinerant electronlike spin fluctuations were observed in an NMR measurement for GaV_4S_8, owing to the transfer of d electrons in the cluster in spite of insulating intercluster coupling [3]. Similarly, the organic systems, κ-(BEDT-TTF)$_2$Cu$_2$(CN)$_3$ [4,5] and β'-(BEDT-TTF)$_2$ICl$_2$ [6], which have magnetic molecular dimers, show unconventional ferroelectricity owing to charge fluctuations in the cluster.

Recently, we have turned our attention to a magnetic cluster based insulator, $La_3Re_2O_{10}$. It crystallizes in a monoclinic structure with the space group of $C2/m$, and the lattice parameters are $a = 7.901$ Å, $b = 7.866$ Å, $c = 7.115$ Å, and $\beta = 115.44°$. Here, $La_3Re_2O_{10}$ consists of discrete cluster units, in which two Re atoms in the unit cell are crystallographically equivalent. The Re-Re distance of 2.48 Å within the cluster is substantially shorter than that between clusters, reflecting on strong metal-metal bonding within a cluster. In the ionic model, the formal oxidation state of Re is +5.5, and hence an Re_2 cluster has three $5d$ electrons. Since the point symmetry at the center of Re_2 clusters is D_{2d}, the Re_2 cluster has nondegenerated cluster orbitals. Three $5d$ electrons in the Re_2 cluster occupy these orbitals, resulting in one unpaired spin per one Re_2 cluster. These Re_2 clusters in $La_3Re_2O_{10}$ make a quasi-two-dimensional La^{3+}-$[Re_2O_{10}]^{9-}$ layer, as shown in the bottom inset of Fig. 1. In a layer, the Re_2 clusters form a distorted triangular lattice as shown in the upper inset of Fig. 1. Then, the La^{3+}-$[Re_2O_{10}]^{9-}$ layer and the nonmagnetic lanthanum layer are stacked alternately. Basic magnetic properties of $La_3Re_2O_{10}$ were reported by Cuthbert *et al.* [7]. The temperature dependence of the magnetic susceptibility χ obeys the Curie-Weiss law at high temperatures with an effective paramagnetic Bohr magneton number of $p_{\rm eff} = 1.63$ per formula unit, which is near the value for a free ion with $S = 1/2$. Below ~150 K, the χ deviates from the Curie-Weiss law and shows a broad peak and a shoulder, whereas χ of field-cooled trace has only one broad maximum. In addition, χ shows a sharp cusp at $T = 18$ K, although origins of these anomalies are not clarified.

In this paper, we report the total magnetic properties and the magnetic phase diagram of $La_3Re_2O_{10}$. We found that $La_3Re_2O_{10}$ shows several sets of the successive phase transition with an unconventional multicritical point on the magnetic field-temperature phase diagram. We propose that such unconventional phenomena are originated in the characteristics of the cluster magnet.

II. EXPERIMENTAL METHODS

Polycrystalline samples of $La_3Re_2O_{10}$ were prepared using a solid state reaction method. The mixture of starting materials, La_2O_3, ReO_2, and ReO_3, in an appropriate molar ratio was heated at 1050 °C for 40 hours in a sealed evacuated silica tube. The starting materials ReO_2 and ReO_3 were purified before use. This process is an important key of synthesizing high quality samples of $La_3Re_2O_{10}$. By means of x-ray diffraction measurements, the obtained sample was found to be in a single phase.

The magnetization was measured under several magnetic fields up to 7 T by using a magnetic property measurement system (MPMS; Quantum Design) equipped in Research Center for Low Temperature and Materials Sciences, Kyoto University. The temperature dependence of the specific heat was measured using a conventional relaxation method under applied magnetic fields up to 14 T with a physical property measurement system (PPMS; Quantum Design).

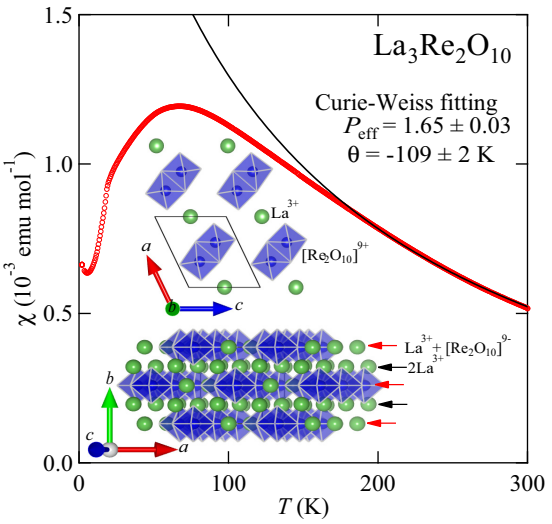

FIG. 1. (Color online) Magnetic susceptibility under the applied magnetic field of 0.1 T in $La_3Re_2O_{10}$. The blue solid line shows the result of Curie-Wiess fitting in the high-temperature region, which gives $\theta_W = -109 \pm 2$ K and $p_{\rm eff} = 1.65 \pm 0.02$ per Re_2 cluster. The upper inset shows the crystal structure of $La_3Re_2O_{10}$ perpendicular to the ac plane. Blue polyhedra and green balls denote $[Re_2O_{10}]^{9-}$ clusters and La^{3+} ions, respectively. The bottom inset shows the layer structure in $La_3Re_2O_{10}$ stacked along the b axis. Red and black arrows show the La^{3+}-$[Re_2O_{10}]^{9-}$ layer and the La^{3+} layer, respectively.

III. RESULTS AND DISCUSSION

In the previous study [7], the data of the magnetic susceptibility $\chi = M/H$ after being zero-field cooled (ZFC) show two broad maxima at 55 and 105 K, whereas those after being field cooled (FC) show only a single peak at 60 K. Figure 1 shows the temperature dependence of χ in our high-quality polycrystalline sample. In the present study, only one broad maximum without any hysteresis is observed approximately at 60 K both in ZFC and FC traces. Thus the temperature hysteresis and the peak at 105 K in the previous study might be extrinsic owing to some impurities or defects.

At high temperatures, χ is well fitted by the Curie-Weiss formula with the Weiss temperature $\theta_{\rm W}$ of -109 ± 2 K and the effective Bohr magneton number $p_{\rm eff}$ of 1.65 ± 0.02 per one Re_2 cluster. These values are very similar to those of the previous report [7]. The $p_{\rm eff}$ value is close to the expected spin-only contributed value of 1.73 for $S = 1/2$. Negative $\theta_{\rm W}$ indicates the presence of antiferromagnetic interactions among spins of Re_2 clusters. In the low-temperature region, χ has a maximum around $T = 60$ K, suggesting the development of short-range ordering among spins of Re_2 clusters owing to the low dimensionality and/or the spin frustration. A steep drop of χ at $T_N = 18.7$ K indicates an antiferromagnetic ordering. The small enhancement of M/H below 10 K is due to the small amount of magnetic impurities or defects. This is much smaller than that of a previous report [7], indicating that our sample has higher quality. The value of M/H extrapolated to 0 K decreases to approximately two-thirds of that just above the transition, which is a typical behavior for three-dimensional antiferromagnetism of the polycrystalline sample. This fact indicates that the antiferromagnetic ordering occurs at $T_{\rm N}$. The ratio $f = |\theta_{\rm W}/T_N|$, which ordinary describes the strength of spin frustration, is estimated to be $f = 5.86$. This rather large value suggests the presence of low-dimensional antiferromagnetic correlation or some spin frustration. This is consistent with the development of the short-range ordering, which is observed as the broad maximum in χ.

In order to clarify the origins of this short-range ordering in $La_3Re_2O_{10}$, we analyzed the temperature dependence of χ using several spin models. First, we discuss the behavior of χ using the $S = 1/2$ uniform Heisenberg antiferromagnetic chain model with so-called Bonner-Fisher equation [8],

$$\mathcal{H} = -2J_{\rm 1D} \sum_i \boldsymbol{S}_i \cdot \boldsymbol{S}_{i+1}, \qquad (1)$$

where $J_{\rm 1D}$ is the nearest-neighbor exchange interaction. The calculated χ is not in good agreement with χ of $La_3Re_2O_{10}$ as shown in Fig. 2. The red broken and chained lines in Fig. 2 show the curves with $J_{\rm 1D} = -50.5$ and -74 K, respectively. As can be seen in Fig. 2, in the case of $J_{\rm 1D} = -74$ K, the Bonner-Fisher χ almost coincides with that of $La_3Re_2O_{10}$ only in the high-temperature region. However, the temperature at which χ has a maximum is much higher than the actual χ of $La_3Re_2O_{10}$. On the other hand, when we attempted to reproduce the temperature at which χ is maximum, we found that the interaction should be $J_{\rm 1D} = -50.5$ K. In this case,

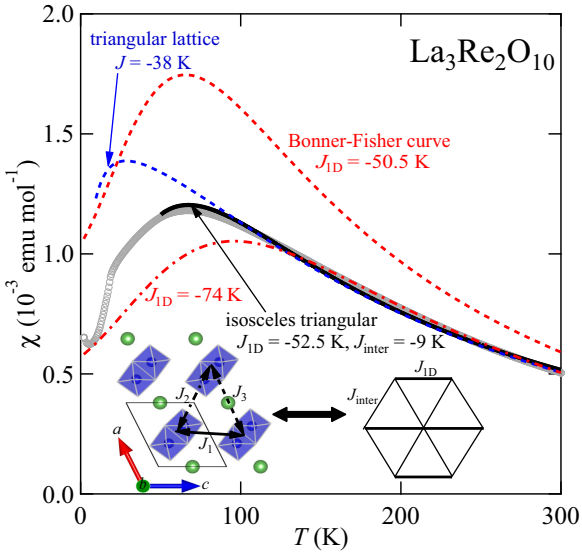

FIG. 2. (Color online) Comparison between spin models and measured χ in $La_3Re_2O_{10}$. Red broken and chained lines show the calculated χ using $S = 1/2$ uniform Heisenberg antiferromagnetic chain (so-called Bonner-Fisher curve [8]) with exchange coupling $J_{\rm 1D} = -50.5$ K and that with -74 K, respectively. The black solid curve shows the calculated χ using eighth-order high-temperature expansions [9] of $S = 1/2$ Heisenberg isosceles triangular lattice model with exchange coupling $J_{\rm 1D} = -52.5$ K and $J_{\rm inter} = -9$ K. The blue broken line shows the result using fourteenth-order high-temperature expansions of $S = 1/2$ Heisenberg isosceles triangular lattice model [10] with the exchange interaction of $J = -38$ K. The left inset shows exchange pathways J_1, J_2, and J_3 among Re_2 clusters on the ac plane in $La_3Re_2O_{10}$. The right inset shows the simplified spin model of isosceles triangular lattice of $La_3Re_2O_{10}$.

there are large deviations between calculated and measured χ. Thus we introduce the interchain interaction to the above model. In the crystallographic ac plane of $La_3Re_2O_{10}$, there are three kinds of nearest neighbor exchange interactions J_1, J_2, and J_3 among the cluster spins as shown in the left inset of Fig. 2. For simplicity, we introduce an isosceles triangular lattice model,

$$\mathcal{H} = -2J_{1D}\sum_{i,j} \boldsymbol{S}_{i,j}\cdot\boldsymbol{S}_{i+1,j} - 2J_{inter}\sum_{i,j}(\boldsymbol{S}_{i,j}\cdot\boldsymbol{S}_{i,j+1} + \boldsymbol{S}_{i,j}\cdot\boldsymbol{S}_{i+1,j+1}), \quad (2)$$

which consists of the large exchange interaction J_{1D} and the small J_{inter} in a triangle as shown in the right inset of Fig. 2. The calculated χ using the eighth-order high-temperature expansions of this isosceles triangular lattice Heisenberg antiferromagnetic model [9] with the exchange interaction parameters $J_{1D} = -52.5$ K and $J_{inter} = -9$ K is denoted by the black solid line in Fig. 2. This does reproduce well the measured χ of $La_3Re_2O_{10}$. For comparison, the calculated χ using the fourteenth-order high-temperature expansion in a regular triangular lattice Heisenberg antiferromagnetic (TAFM) model [10] ($J = -38$ K) is shown by the blue line in Fig. 2. The calculated χ of TAFM does not agree with the measured χ at all. These facts suggest an existence of the large exchange interaction J_{1D} as a quasi-one-dimensional chain and small interchain interactions J_{inter} on the ac plane. Although this model does not answer the question of which exchange interaction ($J_1 \sim J_3$) corresponds to J_{1D}, it is speculated that J_1 corresponds to J_{1D} by considering the number of exchange pathway among Re_2 clusters.

Next, we discuss the relationship between this isoscales triangular lattice model and the crystallographic arrangement. In $La_3Re_2O_{10}$, when an one-dimensional J_{1D} chain is formed in a direction of $[h,k,l]$, another 1D chain toward $[h,\bar{k},l]$ would be produced owing to the mirror plane perpendicular to the b axis according to the space group of $C2/m$. To make an one-dimensional chain, the direction of $[h,k,l]$ and $[h,\bar{k},l]$ should be equivalent, which corresponds to $k = 0$ or $h = l = 0$. The 1D chain must lie on the ac plane (namely, $k = 0$). In a similar way, a weak interchain exchange interaction J_{inter} should be on the ac plane.

As mentioned above, under low magnetic fields, the magnetic transition at T_N seems to be a conventional behavior of 3D antiferromangetic ordering. On the other hand, we observed signs of the development of low-dimensional correlation and/or spin frustration among the cluster spins. To clarify the magnetic behaviors of $La_3Re_2O_{10}$ at low temperatures, we have measured the temperature dependence of the magnetization under several external fields. In Fig. 3, the M/H values of $La_3Re_2O_{10}$ under various magnetic fields are plotted as a function of T. Below T_N, we observed two anomalies with thermal hysteresis in the case of $H = 1$ T, indicating a first-order transition, while only one anomaly was observed above $H = 2$ T. These transition temperatures T_s and $T_{s'}$ (only in the case of $H = 1$ T) are defined as the infection point in $d(M/H)/dT$ curves. Above $H = 1$ T, the anomaly at $T_{s'}$ was not observed, and T_s increases gradually with increasing the external field. T_s seems to merge with

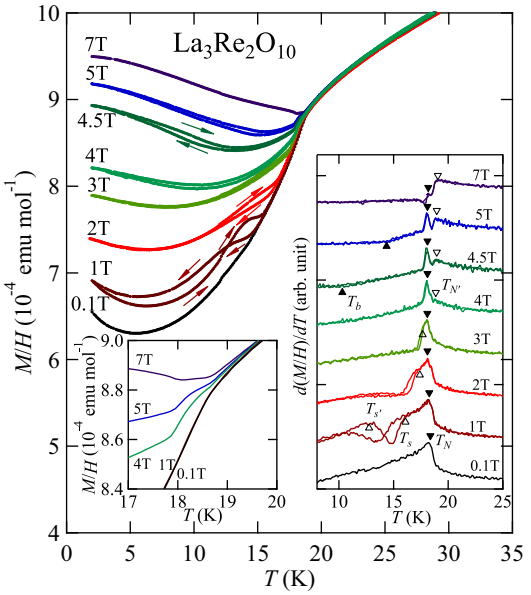

FIG. 3. (Color online) The main panel shows the temperature dependence of the magnetization divided by the external field M/H in $La_3Re_2O_{10}$ measured at several magnetic fields. Below $T_N = 18.7$ K, M/H curves show articulate magnetic field dependence. Under low magnetic fields, no anomaly is observed, however, above $H = 1$ T, an anomaly with a thermal hysteresis is observed. The left inset shows the enlarged view near T_N. The right inset shows $d(M/H)/dT$ vs T. Solid and open down triangles indicate T_N and $T_{N'}$, respectively, and open up triangles indicate T_s (and $T_{s'}$ only in the case of $H = 1$ T). T_b is the bending temperature of $d(M/H)/dT$ indicated by solid up triangles.

T_N around $H = 4$ T. On the other hand, above $H = 4$ T, an extra peak, which is indicative of the phase transition, is observed in $d(M/H)/dT$. We assign the temperature at which $d(M/H)/dT$ exhibits the peaked anomaly above $H = 4$ T as $T_{N'}$. With increasing the applied field, at first T_N decreases below $H = 5$ T, then increases above $H = 5$ T. In addition, considering the extinction of the anomaly at T_s above $H = 4$ T, the field-induced phase seems to exist.

The strong magnetic field dependence of M/H and various magnetic transitions were observed in the magnetic measurement in $La_3Re_2O_{10}$. In order to discuss these magnetic phase transitions in thermodynamics, we measured the specific heat C of $La_3Re_2O_{10}$. Figure 4 shows the temperature dependence of the specific heat divided by temperature (C/T) without the external magnetic field. The lambda-shaped peak seems to be split into two peaks at $T_N = 18.20$ K and $T_{N'} = 18.45$ K. With applying the magnetic field up to 4 T, these peaks become broad, then peaks sharpen again with enlargement of the peak splitting above 6 T, as shown in the inset of Fig. 4. Above $H = 6$ T, both T_N and $T_{N'}$ rise with increasing H. These anomalies are observed without external field, which indicates that the magnetic anisotropy is not the origin of the peak splitting. We confirmed such anomalies by using another batch of samples. There exists no detectable anomaly at T_s in the temperature dependence of C/T. According to the Clausius-Clapeyron equation, the magnetic entropy change ΔS at the first-order transition is in proportion to the increment

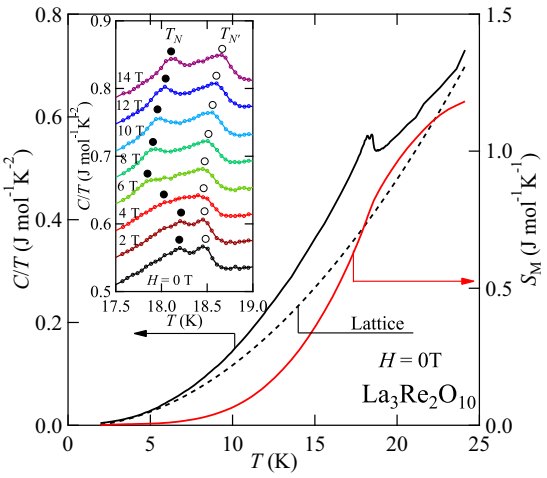

FIG. 4. (Color online) Temperature dependence of the heat capacity divided by temperature C/T of $La_3Re_2O_{10}$. The dashed line is the lattice contribution estimated by fitting with $C/T = \beta T^2$ within the low-temperature range below 5 K. The magnetic entropy S_M is plotted after subtraction of the lattice contribution. The inset shows C/T between 17.5 and 19 K under various fields. Each curve is displaced vertically upward by 0.04 J mol^{-1} K^{-2} with increasing external field by the step of 2 T. Solid and open circles indicate T_N and $T_{N'}$, respectively.

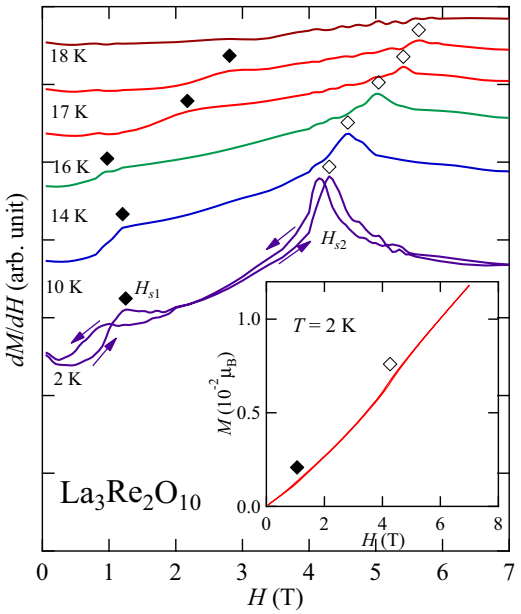

FIG. 5. (Color online) Magnetic field dependence of the differential magnetization dM/dH in $La_3Re_2O_{10}$ at various temperatures up to $H = 7$ T. Solid and open diamonds indicate the transition fields H_{s1} and H_{s2}, respectively. The inset shows the magnetization process at $T = 2$ K.

of magnetization ΔM. Since ΔM is very small at T_s, the latent heat accompanied with the first-order transition at T_s is thought to be small. For this reason, an anomaly at T_s cannot be detected as an entropy change in this case.

The magnetic entropy S_M is calculated by integrating C/T after subtraction of the estimated lattice contribution by fitting with $C/T = \beta T^2$ below 5 K. The total magnetic entropy deriving from $S = 1/2$ should be $R \ln 2 = 5.76$ J mol^{-1} K^{-1}. Here, at T_N, S_M reaches approximately 0.79 J mol^{-1} K^{-1}, which is 14 % of the total magnetic entropy. Since the magnetic entropy changes accompanied with the magnetic long-range ordering are very small, the intercluster short-range orderings are developed above T_N, which should be attributed to the low-dimensional nature and/or spin frustration effects.

Although the behavior of M/H under $H = 0.1$ T seems to be typical for antiferromagnets, unconventional several phase transitions are observed in the higher magnetic field. In addition, we observed a nonmonotonic temperature dependence of T_N, that is, T_N increases with increasing field up to $H = 6$ T and decreases above $H = 6$ T, which is found in the temperature dependence of C/T. These facts suggest the existence of new field-induced phases in $La_3Re_2O_{10}$. To clarify details of magnetic orderings in $La_3Re_2O_{10}$, we have measured the magnetization M as a function of the magnetic field H.

Figure 5 shows the differential magnetization (dM/dH) measured at various temperatures (M measured at $T = 2$ K is in the inset panel). Steps in dM/dH can be seen at H_{s1} and H_{s2} with hystereses indicated by the solid and open diamonds. These behaviors are possibly owing to first-order spin-flop transitions. The transition field H_{s2} monotonically increases with increasing temperature. On the other hand, the temperature dependence of H_{s1} is different from that of H_{s2}. At low temperatures, H_{s1} slightly decreases with increasing temperature. Then, H_{s1} seems to have a local minimum at $T = 16$ K. H_{s1} shows a steep increase above $T = 16$ K, and finally H_{s1} comes to merge with H_{s2}. No distinct anomaly at H_{s2} was observed in the measurement of the temperature dependence of M/H. However, $d(M/H)/dT$ curves in the cases of $H = 4.5$ and 5 T swerve at $T_b \sim 10$ and ~ 15 K represented by solid up triangles in the inset of Fig. 3. These anomalies are attributed to the first-order transition occurring at H_{s2}. As a preliminary study, magnetization measurements were performed in the field up to 60 T at $T = 4.2$ K, where the Re_2 cluster magnetic moment is 0.12 μ_B. The moment is quite small compared with the full saturation moment of 1 μ_B. Thus the energy scale of the low-dimensional short-range ordering, which is developed from high temperatures, is thought to be much higher than 60 T.

Here, we summarize the magnetic phase transitions observed in the magnetization and the specific heat measurements to construct the magnetic field-temperature (H-T) phase diagram of $La_3Re_2O_{10}$ as shown in Fig. 6. The slope of the phase boundary line between the antiferromagnetic (AFM) and the intermediate-field (IF) phases has a minimum at $T \sim 15$ K. The successive phase transition at $T_{s'} = 12.7$ K and $T_s = 15.3$ K in $H = 1$ T can be explained as the reentrant transition(s); in the heating process under $H = 1$ T, the AFM $\rightarrow$ IF transition occurs at $T_{s'} = 12.7$ K and the IF $\rightarrow$ AFM transition at $T_s = 15.3$ K. This picture agrees with the fact that the value of magnetic susceptibility in the heating process is higher than that in the cooling process between $T_{s'}$ and T_s, and below $T_{s'}$ the large/small relation of magnetic susceptibility is reversed.

Two consecutive phase transitions were observed at $T_N = 18.20$ K and $T_{N'} = 18.45$ K, respectively, without the external

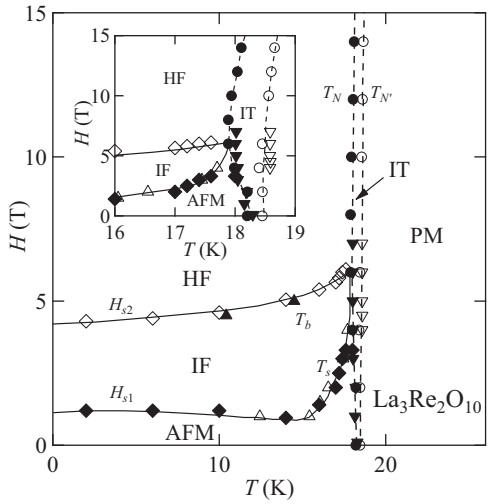

FIG. 6. Magnetic field-temperature phase diagram of $La_3Re_2O_{10}$ determined from the results of the temperature and field variations of the magnetization and the specific heat. Triangles, diamonds, and circles symbols represent the points with anomalies obtained by the measurement of M/H vs T, M vs H, and C/T vs T, respectively. The solid and broken lines describe first- and second-order transitions, respectively. The abbreviations used are as follows: PM, paramagnetic phase; IT, intermediate-temperature phase; AFM, antiferromagnetic phase; IF, intermediate-field phase; HF, high-field phase.

magnetic field. With increasing the external magnetic field, the difference in temperature between T_N and $T_{N'}$ becomes large. The entropy changes at T_N and $T_{N'}$ are very small compared with that of conventional magnetic long-range orderings. From this fact, we speculate that the intermediate temperature phase (IT) between T_N and $T_{N'}$ is a partially ordered phase induced by frustration effect. Similarly, consecutive transitions and the partial ordering were observed in a spinel oxide $GeNi_2O_4$ [11]. The temperature dependence of χ is well reproduced by the $S = 1/2$ isosceles triangular lattice model ($J_{1D} = -52.5$ K and $J_{inter} = -9$ K) in the ac plane of $La_3Re_2O_{10}$. In this spin model, the spin frustration is effective. Thus a partial ordering in the IT phase is possibly realized in $La_3Re_2O_{10}$.

The phase diagram has an unconventional multicritical point located at ($H_c = 6$ T, $T_c = 17.8$ K), where two first- and two second-order lines converge. Although ordinary in $S = 1/2$ spin systems, the magnetic anisotropy is small, the present phase diagram would be made by a superposition of phases in all magnetic field directions because our measurements were performed on polycrystalline samples. The complete phase diagram considering the magnetic anisotropy cannot be constructed in the present stage. Even if each IF and HF phase appear independently in the $H(\theta,\phi)$-T phase diagram, the multicritical point would exist in the phase diagram. It is necessary to synthesize the single crystal of $La_3Re_2O_{10}$ in order to solve the problem, and it is a future issue. Anisotropic spin-flop behavior will give a degree of freedom for the external magnetic field direction. Several intensive studies of multicritical phenomena were done in the investigation field of the anisotropic antiferromagnet [12–21]. The external magnetic field applied to the anisotropic antiferromagnet on the bipartite lattice along the spin easy axis leads to the first-order spin-flop transition with the emergence of a bicritical point. Such a bicritical point can be explained by the Landau phenomenological theory of the competition between two order parameters [12,13]. Simultaneously, this theory also suggested that a new intermediate phase between antiferromangetic and spin-flop phases could appear and then the bicritical point would become a tetracritical point where four second-order lines converge. For example, K_2MnF_4 [14] and $RbMnBr_3$ [15–17] show the multicritical behaviors based on this theory. However, like the case of $CsNiCl_3$, an H-T phase diagram sometimes shows a novel multicritical point that cannot be explained by the Landau phenomenological theory [18]. In the case of $CsNiCl_3$, the multicritical point lies at the cross point of a first-order and three second-order transition lines. This criticality can be explained by a scaling theory considering the spin chirality and the spin frustration effect [19,20]. The multicritical point found in $La_3Re_2O_{10}$ is located at the crosspoint of two first- and two second-order lines. Such a multicritical phenomenon cannot be interpreted only by the magnetic interactions and magnetic anisotropy, suggesting a presence of other degrees of freedom.

Since the Re_2 cluster has nondegenerated cluster orbitals, there is no orbital degree of freedom in $La_3Re_2O_{10}$. Hence two kinds of degrees of freedom possibly contribute to make the multicritical point. As mentioned above, this compound has the spin frustration effect. Thus the spin frustration and an incident spin chirality possibly make many magnetic phases and the unconventional multicritical phenomenon. The other possible factor is the charge degree of freedom owing to the transfer of the d electrons in the Re_2 cluster. For example, in the organic system κ-(BEDT-TTF)$_2$Cu$_2$(CN)$_3$, which has $S = 1/2$ spin per molecular dimer unit, the dipolar-liquid state is realized by the charge degree of freedom in a cluster [4,5]. In the case of β'-(BEDT-TTF)$_2$ICl$_2$, an anomalous ferroelectricity can be attributed to the charge disproportionation within a cluster [6]. Similarly, in the case of $La_3Re_2O_{10}$, there could be the charge degree of freedom in a cluster owing to the formation of the cluster orbital. It is noted that such a charge fluctuation can collaborate with the spin frustration, and finally leads to an exotic multicriticality as characteristics of cluster magnets.

IV. CONCLUSION

Utilizing a high quality polycrystalline sample of $La_3Re_2O_{10}$, successive phase transitions were discovered under magnetic fields. It was also revealed that temperature derivative transitions occur as multistep magnetic orderings. From systematic studies, we constructed a precise H-T phase diagram and found an unconventional multicritical point. Since this multicritical phenomenon cannot be interpreted solely by the magnetic interaction, the spin frustration and/or the charge fluctuation would play important roles. We believed that these successive phase transitions in $La_3Re_2O_{10}$ are caused by characteristics of the cluster magnets.

ACKNOWLEDGMENTS

This work was supported by Grants-in-Aid for Scientific Research from the Japan Society for Promotion of Science (23550152 and 26410089).

[1] R. Pocha, D. Johrendt, and R. Pöttgen, Chem. Mater. **12**, 2882 (2000).
[2] H. Müller, W. Kockelmann, and D. Johrendt, Chem. Mater. **18**, 2174 (2006).
[3] H. Nakamura, H. Chudo, and M. Siga, J. Phys.: Condens. Mater. **17**, 6015 (2005).
[4] M. Abdel-Jawad, I. Terasaki, T. Sasaki, N. Yoneyama, N. Kobayashi, Y. Uesu, and C. Hotta, Phys. Rev. B **82**, 125119 (2010).
[5] C. Hotta, Phys. Rev. B **82**, 241104(R) (2010).
[6] S. Iguchi, S. Sasaki, N. Yoneyama, H. Taniguchi, T. Nishizaki, and T. Sasaki, Phys. Rev. B **87**, 075107 (2013).
[7] H. L. Cuthbert, J. E. Greedan, I. Vargas-Baca, S. Derakhshan, and I. P. Swainson, Inorg. Chem. **46**, 8739 (2007).
[8] J. C. Bonner and M. E. Fisher, Phys. Rev. **135**, A640 (1964).
[9] H. J. Schmidt, A. Lohmann, and J. Richter, Phys. Rev. B **84**, 104443 (2011).
[10] M. Tamura and R. Kato, J. Phys.: Condens. Matter **14**, L729 (2002).
[11] M. K. Crawford, R. L. Harlow, P. L. Lee, Y. Zhang, J. Hormadaly, R. Flippen, Q. Huang, J. W. Lynn, R. Stevens, B. F. Woodfield, J. Boerio-Goates, and R. A. Fisher, Phys. Rev. B **68**, 220408(R) (2003).
[12] K. S. Liu and M. Fisher, J. Low Temp. Phys. **10**, 655 (1973).
[13] M. E. Fisher and D. R. Nelson, Phys. Rev. Lett. **32**, 1350 (1974).
[14] C. A. M. Mulder, H. L. Stipdonk, P. H. Kes, A. J. van Duynevelt, and L. J. de Jongh, Physica B **113**, 380 (1982).
[15] S. Kawano, Y. Ajiro, and T. Inami, J. Magn. Magn. Mater. **104**, 791 (1992).
[16] T. Kato, T. Ishii, Y. Ajiro, T. Asano, and S. Kawano, J. Phys. Soc. Jpn. **62**, 3384 (1993).
[17] L. Heller, M. F. Collins, Y. S. Yang, and B. Collier, Phys. Rev. B **49**, 1104 (1994).
[18] M. L. Plumer, K. Hood, and A. Caillé, Phys. Rev. Lett. **60**, 45 (1988).
[19] H. Kawamura, A. Caillé, and M. L. Plumer, Phys. Rev. B **41**, 4416 (1990).
[20] H. Kawamura, J. Phys.: Condens. Matter **10**, 4707 (1998).
[21] K. Ohgushi and Y. Ueda, Phys. Rev. Lett. **95**, 217202 (2005).